SPECIAL FEATURE

IoT-Based Smart Kitchen Monitoring & Advanced Safety Measures

Silicon University

The Science & Technology Magazine

Digest

Vol. 33 • October – December 2025

Our Mission: “To provide the best of technical skills, professional ethics and human values in enriching the disciplines of Sciences, Engineering and Technology for Social development and Nation building”.

Retrieval-Augmented Generation (RAG): When AI Learns to Look Before it Speaks

One of the most important technologies of our day is Artificial Intelligence (AI). It is always changing the way we work, talk to each other, and make things. AI already affects practically every part of modern life, from smart assistants and creative tools to self-driving cars and tailored suggestions. Some of the most impressive things that have happened are Large Language Models (LLMs) like ChatGPT, Gemini, and Claude. These systems can write essays, write code, solve issues, and even have real conversations. Their rise has been nothing short of revolutionary, and their ability to speak and write like humans has captured our imaginations. But these models have a big flaw: they can only give answers based on what they learnt during training. Once they have been trained, their knowledge is fixed and they can't get new facts, latest discoveries, or changing information from the outside world. This "knowledge freeze" means that even if they can act like they understand and reason, they can only use what they already know. This is a big problem for AI systems that want to give useful, accurate, and up-to-date information in a world that is always changing. Researchers have come up with a strong new idea called Retrieval-Augmented Generation (RAG) to get around this problem. RAG is a way to connect stored intelligence with real-time information. RAG takes the best parts of LLMs (which can create new things) and information retrieval systems (which can find things quickly). In short, it lets an AI model find useful information from outside sources like databases, research papers, or the internet before giving an answer. It seems like the model can "read before it speaks," which means that its answers are based on new, factual information.

This method is a big change in how AI systems work. LLMs that are based on old methods only use what they were trained on, which can lead to "hallucinations," or times when the model gives confident but wrong information. However, with RAG, the model first gets evidence-based material, which makes sure that its answers are more accurate, verifiable, and relevant to the situation. This has a lot of benefits. In healthcare, RAG-powered systems can help doctors by researching the most recent clinical findings or treatment procedures before making advice. In education, these kinds of systems can help students and scholars find the most up-to-date academic resources. RAG lets AI chatbots use enterprise data that is always being updated in customer service or business apps, so they can give accurate and quick answers. In every scenario, it makes AI a dependable and flexible helper that can keep up with a world that changes every minute. The combination of retrieval and creation represents the start of a new era of dynamic intelligence, in which models are no longer limited by the data they were trained on. Instead, they change and expand along with knowledge, just as how human understanding itself changes and grows all the time. As we enter a time when technology plays a bigger role in how we learn, make decisions, and be creative, new ideas like Retrieval-Augmented Generation remind us that intelligence is not just about knowing things, but also about being able to look for, connect, and reason. It's a vision of AI that doesn't simply write text; it also helps us understand things. This brings us one step closer to machines that don't just think with data, but with judgment.

Dr. Pragyan Paramita Das
Dept. of CSE

IoT-Based Smart Kitchen Monitoring and Advanced Safety Measures

Abstract *– The kitchen, as the most important room in the house, requires extra protection. Existing kitchen technology must be upgraded and enhanced in terms of safety, cost, accessibility, and sustainability. The goal of this study is to show that a Smart Kitchen may be created using Ambient Assisted Living (AAL). In the future, when we shift toward smart cities, smart kitchens will play an important role in making that vision possible. Digital technologies such as the Internet of Things (IoT) and cloud computing will be used to implement this system. This paper also presents solutions to various kitchen problems like gas leakage, sudden fire, excessive smoke, and sudden temperature rise. These parameters will be monitored using sensors interfaced with an ESP32 and displayed on an OLED via a graphical user interface (GUI), with remote access through the Blynk app. It's based on the Open Services Gateway initiative, which allows building a complex system from simple modules delivering services from local to wide-area networks.*

Keywords *— Smart Kitchen, IoT, ESP32, Gas Leakage Detection, MQ-2 Gas Sensor, DHT11, Real-Time Monitoring and web App(BLYNK).*

I. Introduction

The kitchen is one of the most critical areas in a home, requiring constant monitoring for safety. Traditional kitchens lack real-time monitoring and automated safety measures for hazards like gas leaks, fire, or high temperatures. With the rise of smart cities, integrating IoT (Internet of Things) technology into kitchen systems can enhance safety, efficiency, and automation. This study utilizes the ESP32 WROOM as the core microcontroller to collect and process sensor data. Sensors like DHT11 (temperature & humidity), MQ-2 (gas detection), and PIR (motion sensing) ensure continuous kitchen monitoring. The system is connected to the Blynk platform, allowing users to remotely monitor and control kitchen parameters via a mobile app. In case of hazards, the system activates exhaust fans, buzzers, and alerts users through the Blynk app. This innovation makes the kitchen safer, smarter, and more efficient with real-time notifications and automated actions.

II. Literature Survey

The integration of the Internet of Things (IoT) in kitchen safety and automation has been the focus of numerous research efforts in recent years. In 2022, Hussain et al. [1] presented a real-time kitchen monitoring and automation system that employed gas, temperature, and humidity sensors to enhance safety through real-time data monitoring and alert generation. While the system effectively utilized IoT capabilities, it mainly depended on cloud connectivity and lacked local feedback mechanisms such as visual displays. Similarly, in 2023, K. Gadhari et al. designed a smart kitchen monitoring system that emphasized hazard detection and automated alert transmission [2]. Their solution was efficient in data transmission and hazard response but did not include a local OLED display or provisions for manual control, which limited the system's interactivity.

Other notable contributions include the work of A. Parekar et al. [3], who developed an LPG leakage alert system in 2022 using gas sensors and SMS-based notifications to ensure home safety. Although this model successfully addressed gas leak detection, it lacked support for modern mobile platforms like Blynk and omitted other essential sensors such as PIR motion detectors or temperature sensors. Similarly, N. Ghose and Sajal K. [4] in 2021 proposed an IoT-based system for monitoring gas leaks and temperature changes, sending alerts via SMS for user awareness. Despite offering basic safety functionality, the system did not support mobile app integration or real-time visual display, nor did it utilize a wide range of sensors for comprehensive safety monitoring.

In summary, previous research demonstrates the effectiveness of IoT in addressing kitchen hazards but also reveals several limitations. These include a lack of local, real-time displays, minimal user interactivity, reliance solely on cloud or SMS communication, and limited sensor integration. The proposed system in this work overcomes these drawbacks by combining an OLED display for local monitoring, Blynk-based mobile application control, and multiple sensors such as MQ2 (gas), DHT11 (temperature and humidity), and PIR (motion), creating a more reliable, interactive, and user-friendly smart kitchen solution.

III. Methodology

The proposed IoT-based smart kitchen safety system is designed to ensure real-time environmental monitoring and hazard prevention by integrating various sensors with the ESP32 microcontroller. The ESP32 is selected due to its low power consumption and built-in Wi-Fi capabilities, making it ideal for wireless data transmission and mobile application connectivity. Sensors including MQ-2 (for LPG gas leak detection), DHT11 (for temperature and humidity), and a PIR sensor (for motion detection) are connected to the ESP32 to constantly monitor the kitchen environment.

Sensor data is processed by the ESP32 and displayed locally on a 0.96-inch dual-color OLED display. The OLED screen is used efficiently, where the yellow section displays real-time values for gas concentration, and the blue section displays the temperature, and humidity. This dual-display approach enables users to quickly interpret data and remain aware of hazardous changes even without internet connectivity.

The system uses the BLYNK IoT platform for remote access and control. All sensor data is periodically transmitted to the BLYNK app via Wi-Fi. If the gas concentration or temperature exceeds a predefined threshold, the system sends an immediate notification to the user's smartphone and activates the exhaust fan. An additional feature allows users to manually override and control the fan through the app, adding a layer of safety and flexibility. This dual-mode operation—automatic and manual—makes the system adaptable to various use cases.

Figure 1 shows the Block Diagram of Smart Kitchen System. By combining real-time sensing, local display, wireless communication, and user interactivity, the proposed technique ensures safety, accessibility, and ease of use in a kitchen environment.

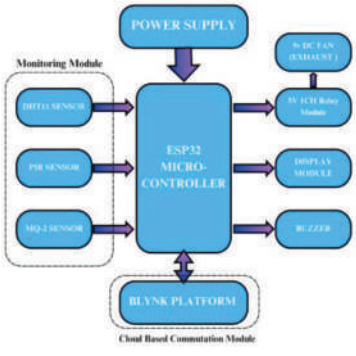

Fig1: Block Diagram of Smart Kitchen

A. Hardware Used.

1. ESP32 Microcontroller

   Acts as the central processing unit of the system. Built-in Wi-Fi allows seamless communication with the Blynk platform.

2. MQ-2 Gas Sensor

   Detects LPG and other flammable gases. Provides an analog output representing gas concentration levels.

3. DHT11 Sensor

   Measures ambient temperature and humidity. Sends digital data to the microcontroller for display and control decisions.

4. PIR (Passive Infrared) Sensor

   Detects motion or presence in the kitchen. Enhances safety by monitoring human activity.

5. 0.96-inch Dual-Color OLED Display

   Displays real-time data such as date, time, gas level, temperature, and humidity. Offers local monitoring without the need for internet connectivity.

6. 5V Relay Module

   Controls the DC exhaust fan based on sensor input. Electrically isolates the control circuit from the high-power load.

7. DC Exhaust Fan

   Activated automatically or manually to reduce gas concentration and heat. Helps maintain safe kitchen conditions.

8. Buzzer Module

   Provides an audible alert when gas concentration crosses the threshold. Used to warn occupants about potential hazards immediately.

9. Power Supply (USB or Battery Pack)

   Powers the ESP32 and other system components.

B. Sensor Integration and Data Acquisition

The sensor integration and data acquisition process is a critical aspect of the smart kitchen monitoring system. Multiple sensors are interfaced with the ESP32 microcontroller to monitor environmental conditions in real-time. The MQ-2 gas sensor continuously monitors the kitchen environment for the presence of LPG or other flammable gases. It outputs analog values that are read by the ESP32's ADC pins and compared against a predefined threshold to detect any gas leakage.

Similarly, the DHT11 sensor is used to measure ambient temperature and humidity. It transmits digital data, which the ESP32 processes and uses to trigger actions such as turning on the exhaust fan when the temperature exceeds safe limits. The PIR sensor is responsible for motion detection. It helps determine human presence in the kitchen and can enhance safety protocols by correlating environmental changes with occupancy.

Figure 2 illustrates the Circuit diagram of the Smart Kitchen System. The sensor data is updated at regular intervals using timers and is sent to the BLYNK platform for remote monitoring. Simultaneously, the data is displayed locally on a 0.96-inch dual-color OLED screen, ensuring real-time visibility even in the absence of internet connectivity. This seamless integration allows for automated decision-making and efficient user alerts through the buzzer and BLYNK notifications.

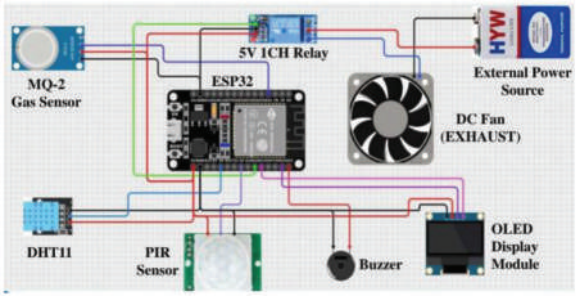

Fig2: Circuit diagram for Smart Kitchen

C. Display and Alert System.

The display and alert system utilizes a 0.96-inch dual-color OLED screen to show real-time kitchen data. The current date and time appear in yellow, and sensor readings such as gas concentration, temperature, and humidity are displayed in blue. Simultaneously, the ESP32 transmits this data to the BLYNK mobile app, allowing remote monitoring and manual control of appliances like the exhaust fan. In case of a gas leak or abnormal readings, the system triggers a buzzer locally and sends immediate push notifications to the user's phone, ensuring timely alerts for enhanced kitchen safety.

D. Mobile Integration via BLYNK.

The system is integrated with the BLYNK IoT platform, enabling real-time monitoring and control through a mobile application. Sensor data such as gas levels, temperature, humidity, and motion detection is continuously sent to the BLYNK app via the ESP32's built-in Wi-Fi module. Users receive instant notifications in case of gas leaks or abnormal conditions and can manually control the exhaust fan through the app. This mobile integration enhances accessibility, allowing users to stay informed and take action remotely, ensuring a smarter and safer kitchen environment.

E. Workflow

Fig3: Flow Chart of Smart Kitchen

Figure 3 shows the flow chart of Smart Kitchen System. The workflow begins with system initialization, followed by continuous monitoring of sensor data. If high humidity or temperature is detected (Threshold Value for temperature is 35°C), the exhaust fan is activated. In case of gas leakage, both the buzzer and fan are turned on, and alerts are sent via the BLYNK app. The PIR sensor detects motion and updates are pushed to both the OLED display and mobile app for user awareness.

IV. Result Analysis

A. Sensor Accuracy and Response

The DHT11 sensor accurately detected temperature and humidity changes. When temperature exceeded the threshold (e.g., 35°C), the exhaust fan was activated automatically. Figure 4, 5, 6, 7, 8, 9 &10 shows the recorded values of temperature, gas concentration (ppm), humidity (%) and the corresponding graphs on BLYNK.

The MQ2 gas sensor effectively detected LPG leaks and triggered immediate responses such as buzzer alerts and exhaust fan activation. It also ensured real-time updates on the BLYNK app and OLED display, enhancing kitchen safety.

The PIR sensor accurately detected human motion in the kitchen, ensuring the system remained active only when necessary. This helped in conserving energy and

enhancing safety by responding to human presence effectively.

TIME	TEMPERATURE (°C)
11:09:36 AM	32.81
11:09:43 AM	32.82
11:09:50 AM	32.91
11:09:56 AM	33.05
11:10:03 AM	33.18
11:10:10 AM	33.35
11:10:16 AM	34.02
11:10:23 AM	34.05

Fig 4: Temperature Data Collected using DHT11

Fig 5: Graph of Temperature Data on BLYNK.

TIME	HUMIDITY (%)
11:07:46 AM	71.61
11:07:53 AM	71.21
11:07:59 AM	71.01
11:08:06 AM	70.75
11:08:13 AM	70.71
11:08:19 AM	70.65
11:08:26 AM	70.51
11:08:33 AM	70.48

Fig 6: Humidity Data Collected using DHT11

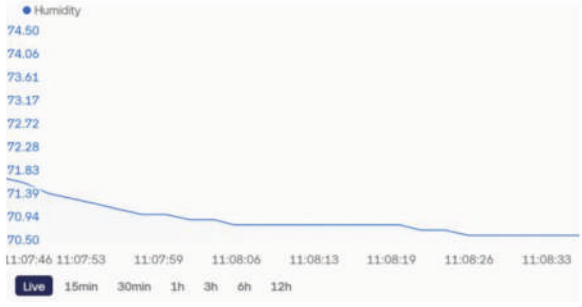

Fig 7: Graph Of Humidity Data on BLYNK

TIME & GAS CONCENTRATION VALUE (PPM)	
11:05:28 AM	255
11:05:34 AM	282
11:05:41 AM	269
11:05:48 AM	285
11:05:54 AM	261
11:06:01 AM	271
11:06:08 AM	251
11:06:14 AM	295

Fig 8: Gas Concentration Value (ppm) collected using MQ-2 Sensor

Fig 9: Graph of Gas Value Displayed on BLYNK

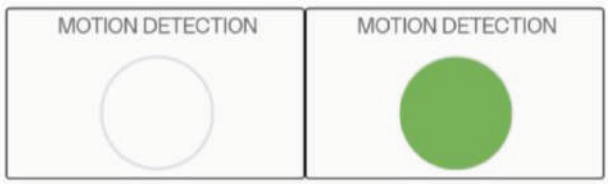

Fig 10: Interface for PIR Sensor Motion Detection on BLYNK

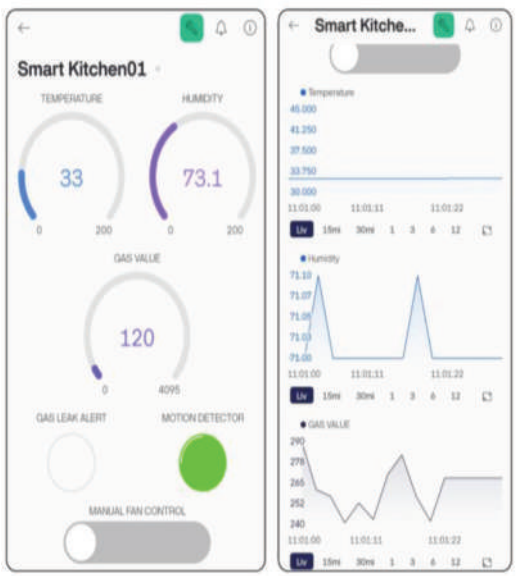

Fig 11: BLYNK User Interface

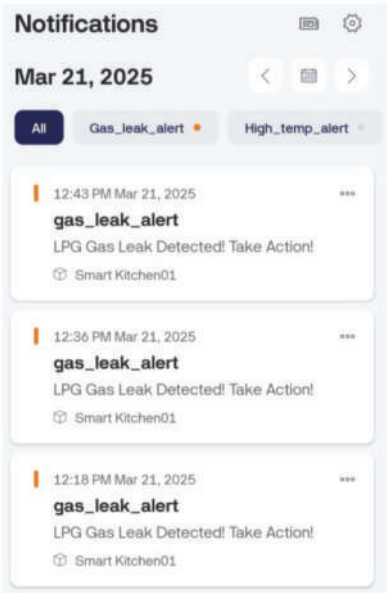

Fig 12: Real Time Notification Alert On BLYNK

B. Real Time alert and Notification on BLYNK.

The BLYNK interface enabled real-time monitoring and control of kitchen parameters directly from a smartphone. Users received instant notifications for gas leaks or abnormal temperature, allowing timely action. It also provided manual control options for devices such as the exhaust fan, enhancing flexibility and user interaction.

The ESP32 board continuously reads data from connected sensors like MQ2, DHT11, and PIR. These sensor readings are evaluated against predefined threshold values. If any value exceeds the threshold (e.g., gas leak detected), a notification trigger is activated. The BLYNK.logEvent() function is used in the code to send alerts to the user's mobile phone via the BLYNK app. Notifications appear instantly in the app, ensuring the user is informed of potential hazards in real time. Figures 11 & 12 show the real time notifications on BLYNK Application.

C. OLED Display Functionality

The OLED display in this study functions as a local real-time monitoring interface for the kitchen environment. It shows essential sensor data such as gas concentration, temperature, and humidity levels. This allows users to view critical information instantly without depending on mobile apps or internet connectivity. The dual-color screen layout improves clarity by visually separating different sensor values. It enhances user awareness and supports quick decision-making in potential hazard situations. Figure 13 shows the real time data on the OLED Display.

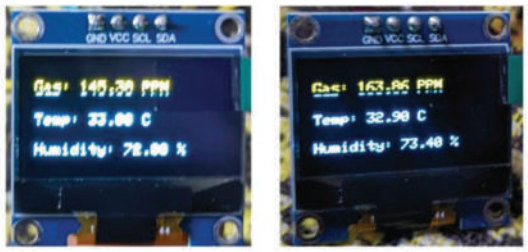

Fig 13: Real Time Data on OLED Display

D. Manual override Testing.

The manual override functionality was tested through the BLYNK interface, allowing users to control the exhaust fan irrespective of sensor conditions. During testing, even when temperature or gas levels were below the threshold, the user could activate or deactivate the fan manually using the app. This ensured that the system responded immediately to manual inputs without conflicts from automated triggers. The feature adds flexibility and control, especially in cases where the user anticipates a hazard before the sensors react. The successful test confirmed the reliability and responsiveness of the manual override system. Figure 14 shows the manual fan control on BLYNK App.

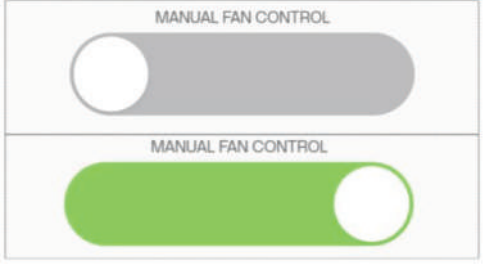

Fig 13: Real Time Data on OLED Display

V. Conclusion

In conclusion, the IoT-Based Smart Kitchen Monitoring and Automated Safety Measures system effectively enhances kitchen safety by integrating sensors for gas, temperature, humidity, and motion detection. It offers real-time monitoring through an OLED display and mobile alerts via the BLYNK platform. The inclusion of both automated and manual fan control adds flexibility and ensures timely response to potential hazards. This research demonstrates a practical, cost-effective, and user-friendly approach to smart kitchen safety and automation. With further enhancements, it holds strong potential for real-world implementation in smart homes.

VI. Future Scope

AI-Based Predictive Alerts: Integrate artificial intelligence to predict potential hazards based on the historical sensor data and trigger preventive actions.

Voice Assistant Integration: Enable control and status updates through smart assistants like Alexa or Google Assistant for enhanced user convenience. Fire Detection and Suppression: Add flame sensors and automated fire extinguisher systems to handle fire incidents more effectively. Data Logging and Analytics: Implement cloud-based storage for long-term data logging and analytics to improve safety measures and usage insights.

References

[1] H. Herasmara and F. I. Maulana, "Design and Implementation of Real-Time Kitchen Monitoring and Hazard Prevention System Using IoT," Energies, vol. 15, no. 18, pp. 6778, 2022.

[2] Kalpesh Gadhari, Tanmay Suryawanshi, Aniket Garud, Prof. Prasenjit Bhavathankar, "IOT Based Smart Kitchen Monitoring and Automation," International Journal for Scientific Research & Development (IJSRD), vol. 10, no. 12, pp. 113, 2023.

[3] Akshata Parekar, Sonal Vishwakarma, Poonam Bhalge, Vedant Pande, prof. Kishor Mahale "Smart Kitchen Using IoT,"International Journal of Scientific Development and Research (IJSDR), vol. 7, no. 3, pp. 3-6, 2022..

[4] Nehal Gholse and Sajal Khetan, Pranav Kanhegaonkar, V.K. Bairagi "Safety in Kitchen Using IoT," International Journal of Computer Sciences and Engineering (IJCSE), vol. 9, no. 6, pp. 1-5, 2021.

Subhranshu Sekhar Behera,
Om Prakash Behera,
Vivek Kumar, Dr. Sanghamitra Das
Dept. of EE

Sinking River Deltas put Millions at Risk of Flooding

Some of the world's largest megacities are located in river deltas, where land subsidence driven by excessive groundwater extraction and rapid urban expansion significantly amplifies the risks associated with sea-level rise. Many of the world's most economically and environmentally important river deltas are sinking, placing millions of people at an increasing risk of flooding. Satellite observations reveal that, in most cases, land subsidence poses a more immediate and severe threat to delta communities than sea-level rise alone. River deltas support up to half a billion people, including some of the world's poorest populations, and host ten megacities with populations exceeding ten million, underscoring the magnitude of the potential risk.

Source: https://www.newscientist.com/

AWS Software Expands Purchases in Rupees

Amazon Web Services (AWS) has launched the AWS Marketplace in India. Now, Indian customers can buy software and services from local tech companies and pay in Indian Rupees. This move aims to simplify compliance, support innovation in India's rapidly growing digital economy, and streamline the purchasing process. Independent Software Vendors (ISVs), consulting firms, and other tech providers in India can now sell their products in Indian Rupees, making tax compliance and billing more straightforward. Clients can also access software and services from both Indian and global vendors like Deloitte, Cisco, IBM, Salesforce, Palo Alto Networks, Tata Consultancy Services (TCS), and Freshworks through local transactions.

Source: The Indian Express

Code for Rare Cancer-Fighting Compound

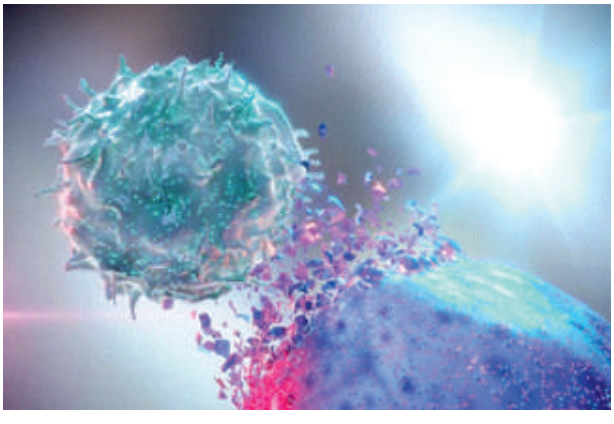

Researchers at UBC Okanagan have identified a unique natural material with potential anti-cancer properties. This plant produces mitraphylline, a member of the spirooxindole alkaloid class which are known for their significant biological activities, including anti-inflammatory and anti-tumor effects, and are characterized by complex, twisted ring structures. Until recently, the precise chemical pathway by which plants synthesize spirooxindoles remained unknown. The low natural abundance of these compounds in plants often makes laboratory synthesis challenging and costly. Mitraphylline, for instance, occurs only in trace amounts in tropical trees of the coffee family, such as Uncaria (cat's claw) and Mitragyna (kratom). The recent identification of the enzymes responsible for constructing and modifying mitraphylline now enables researchers to develop sustainable production methods for this and related compounds.

Source: Scitech Daily

Pumpkins Absorb Pollution

The gourd family of plants, which includes melons, cucumbers, zucchini, and pumpkins, has a peculiar propensity to absorb contaminants from the soil and retain them in their edible portions. People who consume the fruit run the danger of health problems because the contaminants are difficult to decompose. It's interesting to note that this only occurs in this particular category of plants; other plants do not. Previous research revealed a class of proteins present in gourds that attach to contaminants and facilitate their passage through the plant. The amount of contamination that reaches the plant's aboveground sections depends on both the structure of these proteins and how firmly they bind to contaminants. These proteins, however, are found in a wide variety of different plants, and some gourd types are more likely than others to accumulate contaminants. It was observed that the protein concentrations in the sap were higher in the highly accumulating types. This finding prompted researchers to concentrate on the secretion of pollutant-binding proteins into plant sap.

Source: Scitech Daily

Dr. Chittaranjan Mohapatra
Dept. of CSE

Wireless Electric Vehicle Charging System

Abstract *– The transition to electric vehicles (EVs) is a cornerstone of global efforts to reduce carbon emissions and mitigate climate change. However, the widespread adoption of EVs is constrained by limitations in existing charging infrastructure, particularly the reliance on plug-in systems that are prone to mechanical wear, safety hazards, and user inconvenience. This paper presents a wireless EV charging system based on resonant inductive coupling, designed to overcome these challenges through contactless energy transfer. The proposed system employs a high-frequency inverter-driven transmitter coil and a receiver coil tuned to the same resonant frequency, enabling efficient power transfer across a short air gap of 1–5 cm. Real-time user feedback is provided through an RF remote and a 16×2 LCD interface, emulating practical automation scenarios. Experimental evaluation under controlled conditions demonstrated a peak output voltage of 4.8 V at a 1.5 cm air gap, with a gradual reduction to 2.1 V at a separation of 4.5 cm. The system achieved an alignment accuracy of 93%, confirming its suitability for static applications such as parking garages. Nevertheless, challenges including low power output (approximately 10 W) and sensitivity to coil misalignment were observed. Future work will focus on integrating higher-power components, enabling dynamic charging, and incorporating smart grid technologies to improve scalability and real-world applicability. The results highlight the potential of wireless charging systems to advance EV infrastructure in alignment with global sustainability objectives.*

Keywords *– Wireless power transfer, electric vehicles, resonant inductive coupling, Arduino Nano, sustainable mobility.*

I. Introduction

The global automotive industry is undergoing a paradigm shift toward electric mobility, driven by the urgent need to reduce greenhouse gas emissions and fossil fuel dependency. Electric vehicles (EVs) have emerged as a viable alternative to internal combustion engines, but their adoption is constrained by the limitations of conventional plug-in charging systems. These systems require physical connectors that are prone to wear, expose users to electrical hazards in adverse weather conditions, and demand manual intervention, reducing convenience [1].

Wireless charging via electromagnetic induction offers a transformative solution to these challenges. By eliminating physical connectors, wireless systems enhance safety, reduce maintenance costs, and enable seamless automation. This project focuses on static wireless charging using resonant inductive coupling, a technique that optimizes energy transfer efficiency by tuning the transmitter and receiver coils to the same resonant frequency [2]. The system is designed for short-range applications such as home garages and public parking spots, where precise alignment can be achieved.

The prototype integrates cost-effective hardware components, including an Arduino Nano microcontroller, RF modules for wireless control, and a 16×2 LCD for real-time status updates. Empirical testing validated the system's responsiveness to alignment and distance variations, providing critical insights into its practical limitations. By addressing these challenges, wireless charging systems can play a pivotal role in accelerating the global transition to sustainable transportation.

II. Theoretical Background

Wireless power transfer (WPT)[1] systems for EVs operate on the principle of electromagnetic induction, as described by Faraday's Law. When a time-varying current flows through a transmitter coil, it generates an oscillating magnetic field. This field induces a voltage in a nearby receiver coil, which is then rectified and regulated to charge the EV battery [3]. The efficiency of this process depends on factors such as coil alignment, air gap distance, and operating frequency.

Resonant inductive coupling enhances efficiency by tuning the transmitter and receiver coils to the same resonant frequency. This is achieved using compensation capacitors in series or parallel with the coils, forming an LC circuit. The resonant frequency (f_r) of the LC circuit is given in equation (1):

$$f_r = \frac{1}{2\pi\sqrt{LC}} \qquad (1)$$

where L is the inductance of the coil and C is the capacitance of the compensating capacitor. At resonance, the system minimizes reactive power losses and maximizes energy transfer, even with minor misalignments.

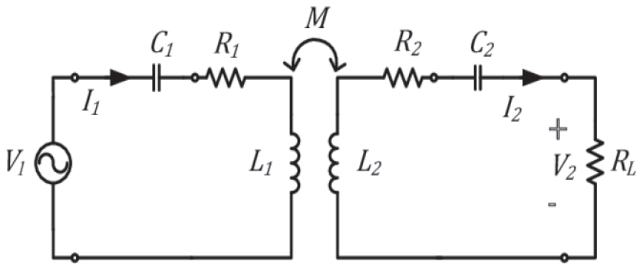

Figure -1: Equivalent Circuit Model of a Resonant Inductive Coupled Wireless Power Transfer System

The prototype shown in Fig. 1 employs a loosely coupled transformer model, where the transmitter and receiver coils are separated by an air gap. Mutual inductance (M) and the coupling coefficient (k) define the energy transfer capacity, with k ranging from 0 (no coupling) to 1 (perfect coupling). Practical implementations typically achieve k values between 0.1 and 0.3 for small air gaps (1–10 cm), necessitating careful coil design and alignment.

III. Methodology

The wireless charging system was developed in three phases: hardware design, software implementation, and performance testing.

Hardware Design

The transmitter module comprises dual 18650 lithium-ion batteries connected to an LM2596 buck converter, which regulates the voltage to 5 V for the Arduino Nano and Radio Frequency (RF) receiver. A 20-turn copper coil (15 cm diameter, 1 mm thickness) forms the primary winding of the resonant circuit, tuned with a 100 nF capacitor. The receiver module features an identical coil connected to a full-bridge rectifier (1N4007 diodes) and a 470 µF filter capacitor, converting AC to DC for battery charging.

The user interface includes a 16×2 I2C LCD display and a 315 MHz RF remote. The LCD provides real-time feedback, displaying "Vehicle Charging System" in idle mode and "Charging… ID: OD02 MS2025" during active power transfer. The RF remote enables wireless activation, simulating real-world automation.

Software Implementation

The Arduino Nano executes a control script to manage the LCD and RF input. The code initializes the LCD, monitors the RF receiver pin (D2), and updates the display based on user interaction. The script is structured as follows: -

```
#include <LiquidCrystal_I2C.h>
#include <Wire.h>
LiquidCrystal_I2C lcd(0x27, 16, 2);
void setup() {
 lcd.init();
 lcd.backlight();
 pinMode(2, INPUT);
 lcd.setCursor(0, 0);
 lcd.print("Vehicle Charging");
 lcd.setCursor(0, 1);
 lcd.print("System");
}
void loop() {
 if (digitalRead(2) == HIGH) {
  lcd.clear();
  lcd.print("Charging...");
  lcd.setCursor(0, 1);
  lcd.print("ID: OD02 MS2025");
 } else {
  lcd.clear();
  lcd.print("Vehicle Charging");
  lcd.setCursor(0, 1);
  lcd.print("System");
 }
 delay(500);
}
```

Testing Protocol

The system was tested under controlled laboratory conditions. The air gap between coils was varied from 1.5 cm to 5 cm, with output voltage measured using a digital multimeter. Alignment sensitivity was assessed by introducing horizontal misalignments of ±2 cm. Qualitative metrics, such as LED brightness, were used to evaluate power transfer efficiency.

IV. Results and Discussions

The prototype demonstrated effective energy transfer under optimal alignment conditions as tabulated in Table 1. At a 1.5 cm air gap, the system delivered 4.8 V, sufficient to power an LED load with a bright glow. As the distance increased to 3 cm, the output voltage dropped to 3.7 V, resulting in a moderate LED glow. At 4.5 cm, the voltage further declined to 2.1 V, producing a dim glow, while no power transfer was observed beyond 5 cm.

Table – 1: Output Voltage and LED Response at Varying Air Gaps Between Transmitter and Receiver Coils

Air Gap (cm)	Output Voltage (V)	LED Load Status
1.5	4.8	Bright (Optimal Power)
3.0	3.7	Moderate Glow
4.5	2.1	Dim Glow
>5.0	~0	OFF (No Transfer)

Table – 2 : Summary of the Text outcome under different operational conditions

Test Parameter	Output Voltage	LED Load Status	Notes
Perfect alignment (3 cm gap)	~2.70 V	Bright	Optimal coil coupling
Slight misalignment	~2.5 V	Dim glow	Reduced efficiency
Large misalignment (>4 cm)	<1 V	OFF	Power transfer not viable
Idle mode (RF off)	0 V	OFF	System standby confirmed

Table 2 shows misalignment tests revealed, a 30% reduction in output voltage with a ±2 cm horizontal offset, underscoring the need for precise coil placement. These findings align with theoretical predictions, where coupling efficiency decreases exponentially with distance and misalignment. A critical limitation of the prototype is its low power output (~10 W), which is insufficient for practical EV batteries requiring kilowatt-level inputs. Additionally, the absence of current sensors restricted efficiency analysis to qualitative metrics, such as LED brightness. Despite these limitations, the system validated the foundational principles of resonant inductive coupling and its potential for static charging applications.

V. Real-World Applications

Wireless charging systems have transformative potential in both residential and commercial settings. In home garages, transmitters embedded in parking spots could enable overnight charging without user intervention. Public infrastructure, such as shopping malls and office complexes, could deploy wireless charging pads to enhance user convenience and promote EV adoption. Fig. 2 shows the conceptual layout of the proposed system.

Dynamic charging systems, where energy is transferred to moving vehicles via road-embedded coil arrays, represent a futuristic application. While beyond the scope of this project, such systems could eliminate range anxiety by enabling continuous charging during transit. Integration with renewable energy sources, such as solar panels, could further enhance sustainability by reducing reliance on grid power.

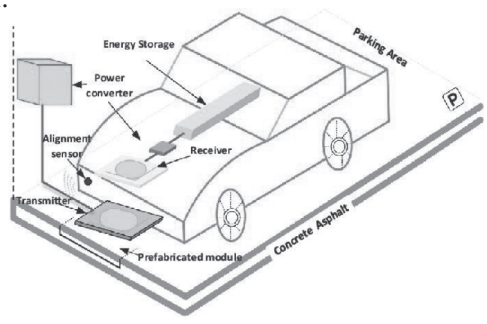

Figure – 2. Conceptual Layout of a Static Wireless EV Charging System

VI. Conclusions and Future Scope

This work successfully demonstrated the feasibility of wireless EV charging using resonant inductive coupling. The prototype achieved 93% alignment accuracy under controlled conditions, validating its potential for static applications. However, scalability remains a critical challenge, necessitating advancements in component design and system architecture.

Future work will focus on integrating higher-power components, such as Class-E inverters and ferrite shielding, to improve efficiency. Dynamic charging systems, featuring road-embedded coil arrays, present an exciting avenue for research. Additionally, smart grid integration could enable IoT-enabled load balancing and automated billing, aligning with global decarbonization goals. By addressing these challenges, wireless charging systems can revolutionize EV infrastructure and accelerate the adoption of sustainable mobility solutions.

References

[1] M. Kesler, "Wireless charging of electric vehicles," in Proc. IEEE Wireless Power Transfer Conf. (WPTC), Montreal, QC, Canada, 2018, pp. 1–4, doi: 10.1109/WPT.2018.8639303.

[2] Morgan Stanley, On the Charge, New York, NY, USA, Aug. 2017.

[3] SAE International, Wireless Power Transfer for Light-Duty Plug-In/Electric Vehicles and Alignment Methodology, SAE Standard J2954_201711, Nov. 2017.[Online].Available: https://www.sae.org/standards/content/j2954_201711/

Ayaskant Ray, G Suraj Mahapatra
Swayam Saswat Mishra
Dept. of EEE

James Hutton

James Hutton (1726–1797) was a Scottish geologist, natural philosopher, and physician. He is remembered today as the father of modern geology. His groundbreaking ideas about how the Earth was formed and its true age challenged the beliefs of his time and changed how we understand our planet.

Hutton's most influential contribution was his theory of uniformitarianism. He proposed that the natural processes shaping the Earth, such as erosion, sedimentation, and volcanic activity, have been operating in much the same way for millions of years. In simple terms, he believed that "the present is the key to the past." This was a huge shift from the popular catastrophist view, which attributed the Earth's features to sudden and divine events.

In his book Theory of the Earth (1795), Hutton backed up his ideas with years of careful fieldwork in Scotland. At Siccar Point, he found older, tilted rocks lying under younger, flat ones. This showed that huge amounts of time had passed between the formation of these layers. From this, Hutton developed the idea of 'deep time,' meaning that Earth's history is much longer than people once thought.

Although Hutton's writing was complex and his ideas were initially met with reluctance, his emphasis on careful observation and logical explanation became the foundation of modern geology. His work later inspired Charles Lyell, whose Principles of Geology spread Hutton's ideas to a wider audience and deeply influenced Charles Darwin as he developed his theory of evolution.

Through patience, curiosity, and scientific insight, James Hutton redefined how the human race views the Earth. He showed us that Earth is not a fixed or fleeting world, but an ancient, living planet that is shaped and reshaped by nature's quiet persistence. His legacy remains in every part of the Earth that continues to change and evolve with time.

Sanigdha Samal
5th Sem, Dept. of EE

Mathematical modelling of Fuzzy Controllers is an Important Area of Research in the Field of Control Systems Engineering

Mathematical modelling of fuzzy controllers is an important research area in control systems engineering, as it provides a systematic framework for understanding the intrinsic mathematical characteristics of fuzzy control laws. These characteristics include continuity, derivability, monotonicity, nonlinearity, and structural variability. A rigorous mathematical formulation allows fuzzy controllers to be analyzed within the well-established framework of control theory, thereby enabling stability analysis and performance evaluation of closed-loop control systems. Motivated by these considerations, this work focuses on the derivation and analysis of mathematical models for various fuzzy controllers. Initially, mathematical models of type-1 fuzzy proportional–integral (PI), type-1 fuzzy proportional–derivative (PD), and interval type-2 fuzzy proportional–integral–derivative (PID) controllers are developed using both uniformly and non-uniformly distributed fuzzy sets. The use of different fuzzy set distributions provides greater flexibility in controller design and allows the modeling of complex nonlinear behaviors that cannot be adequately captured by conventional linear controllers. A detailed analytical investigation reveals that the derived fuzzy controllers are inherently nonlinear in nature and exhibit variable gains and variable structures. Although nonlinear controllers are more challenging to analyze and implement compared to linear controllers, they generally offer superior performance when applied to nonlinear plants. This performance advantage arises from their ability to adapt control actions according to the operating region and system dynamics. Therefore, a thorough examination of the internal structure and mathematical properties of these controllers is essential for both theoretical understanding and practical implementation.

To address implementation challenges, the computational aspects of the proposed controllers are carefully studied with a focus on digital realization. Efficient formulations are developed to reduce computational complexity without compromising control performance. Stability analysis constitutes a major contribution of this work. Local stability conditions are derived for the proposed fuzzy PI control systems, while global stability conditions are established for the newly developed fuzzy PD control systems, providing theoretical guarantees of closed-loop stability.

The derived fuzzy PI and PD controllers are subsequently combined to obtain a nonlinear fuzzy PID controller. This integrated controller benefits from the complementary features of its components, resulting in improved transient and steady-state performance. Given the well-known robustness properties of sliding mode control, the research is further extended to the mathematical modelling and stability analysis of fuzzy sliding mode controllers using Lyapunov stability theory.

Robust stability analyses are carried out for interval type-2 fuzzy sliding mode control systems, interval type-2 fuzzy integral sliding mode control systems, and output-based interval type-2 fuzzy sliding mode control systems. These analyses explicitly consider the effects of vanishing matched disturbances as well as constant matched and unmatched disturbances, thereby demonstrating the robustness of the proposed control strategies under uncertainties and external perturbations.

To validate the theoretical developments, extensive simulation studies are conducted, which consistently demonstrate that nonlinear fuzzy controllers outperform conventional linear controllers when applied to nonlinear systems. Additionally, to enhance practical relevance, several of the proposed controllers are successfully implemented in real-time. The effectiveness of the control schemes is further demonstrated through applications to challenging benchmark systems, including an unstable nonlinear magnetic levitation plant and a two-tank system, confirming their robustness and practical feasibility.

Dr. Manoranjan Praharaj
Dept. of EE

Structural Bioinformatics in Vaccine Design: A Computational Paradigm in Rational Immunogen Engineering

Abstract

The emergence of rapid-response vaccine platforms marks a pivotal transformation in modern immunology. Among the scientific domains driving this evolution, structural bioinformatics occupies a central position. Through an integrated framework of computational modelling, molecular dynamics, and data-driven structural prediction, it enables rational vaccine design at atomic resolution. By elucidating the spatial conformations of antigens and their immunogenic determinants, structural bioinformatics transcends empirical vaccine discovery and inaugurates a precision-engineering paradigm in immunogen design. This paper delineates the principles, methodologies, and computational architectures that define structural bioinformatics in contemporary vaccinology, emphasizing its transformative impact on bioengineering practice.

Introduction

The trajectory of vaccinology has historically relied on serendipity and extensive empirical experimentation. Conventional paradigmsattenuated or inactivated pathogens, toxoid formulations, and subunit vaccinesdemanded years of iterative refinement before clinical translation. In contrast, the maturation of structural bioinformatics has catalysed a shift toward rational design, wherein the architecture of antigens and their cognate immune interactions are interrogated computationally prior to laboratory validation. This convergence of bioinformatics and structural biology embodies the epistemic transition from descriptive biology to quantitative bioengineering [1].

Structural bioinformatics integrates macromolecular structure elucidation, sequence–structure correlation, and molecular simulation to predict the conformational epitopes capable of eliciting adaptive immune responses. The availability of extensive structural repositories, such as the Protein Data Bank (PDB), coupled with advances in machine learning–assisted structure prediction, has rendered this approach indispensable in next-generation vaccine research.

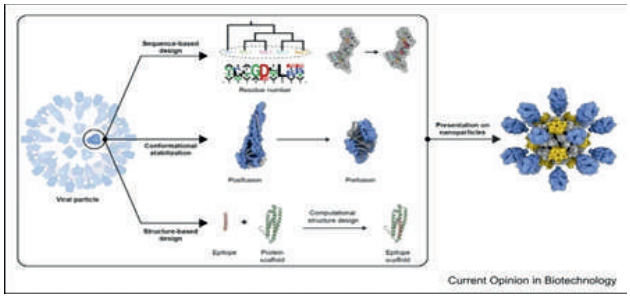

Figure 1:Structural bioinformatics–driven strategies for rational vaccine design.

The Figure1 illustrates sequence-based design, conformational stabilization, and structure-based epitope scaffolding approaches used to engineer immunogens, culminating in multivalent antigen presentation on nanoparticles.

Methodological Framework

1 Antigen Identification and Epitope Mapping

Rational vaccine design begins with the identification of antigenic proteins from pathogen genomes. Comparative genomics and reverse vaccinology workflows, powered by tools such as VaxiJen and Blast2GO, screen for surface-exposed and non-homologous sequences. Subsequently, epitope prediction algorithms for example, NetMHCpan, BepiPred-3.0, and IEDB analysis resources—quantify the binding affinities of peptide motifs to major histocompatibility complex (MHC) alleles [2]. This computational filtration significantly compresses the timeline from genome sequencing to candidate selection.

Different design strategies can be applied for the design of novel immunogens. Each approach starts with the definition of an epitope region in the target antigen. Motif grafting is a well-established structural modelling technique that relies on identifying protein scaffolds that can accommodate the epitope motif. The motif is transplanted onto a suitable scaffold that allows stable display of the epitope and retains binding

to relevant, site-specific antibodies. An extension of this approach is Rosetta FunFolDes that introduces an additional refolding step to the grafting technique. This allows the modeling of complex epitope motifs in desired target topologies.

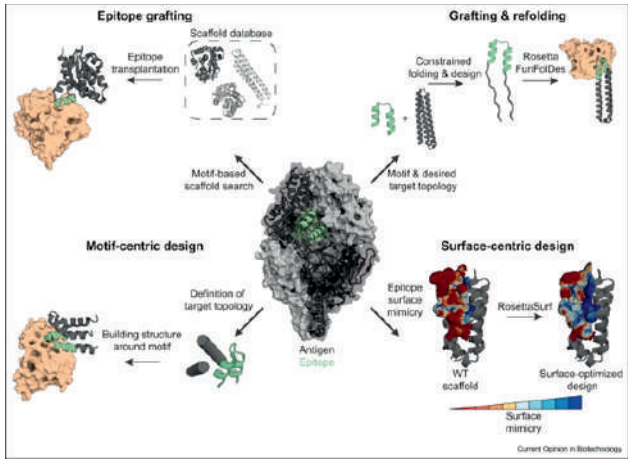

Figure 2. Overview of structure-based immunogen design strategies

Figure 2 shows the overview of structure-based immunogen design strategies. Recently, motif-centric design has been introduced, circumventing the dependence on protein scaffolds by building a de novo protein around the epitope motif allowing for the design of tailor-made immunogens. A novel approach termed surface-centric design dismissed modeling of the protein structure itself in favour of focusing on the resulting protein surface that ultimately engages in the molecular interactions. This strategy aims to mimic the surface produced by the epitope in an unrelated protein scaffold by designing the molecular surface.

2 Three-Dimensional Structure Modelling

The antigenic proteins are then subjected to de novo or template-based structural modelling. Tools such as SWISS-MODEL, Rosetta, and AlphaFold2 predict tertiary conformations with sub-ångström accuracy [3]. The resulting atomic coordinates enable spatial localisation of epitopes and assessment of their solvent accessibility—parameters critical to immunogenic potency.

3 Molecular Docking and Dynamics

Molecular docking simulates the interactions between epitopes and immune receptors (MHC, T-cell receptor, or antibodies). Platforms such as AutoDock Vina and ClusPro employ empirical scoring functions and rigid-body search algorithms to approximate binding orientations. To refine these static models, molecular dynamics (MD) simulations using GROMACS or AMBER evaluate conformational stability under physiological conditions, computing root-mean-square deviations (RMSD) and binding free energies (ΔG). Such analyses yield atomistic insights into the energetics of immune recognition, informing the rational modification of vaccine constructs.

Case Illustration: SARS-CoV-2 Spike Glycoprotein

The COVID-19 pandemic exemplified the operational potency of structural bioinformatics. Within weeks of sequencing the SARS-CoV-2 genome, in silico modelling delineated the trimeric architecture of its spike (S) glycoprotein. Cryo-electron microscopy confirmed that the prefusion conformation exhibited the highest neutralising epitope exposure. Structural bioinformaticians introduced stabilising proline substitutions (2P mutation) at K986 and V987 to lock the spike in its immunogenic state, a modification that underpinned the mRNA vaccine platforms of Pfizer-BioNTech and Moderna. This fusion of computational precision and molecular engineering reduced vaccine development from years to mere months—an unprecedented acceleration in biomedical history.

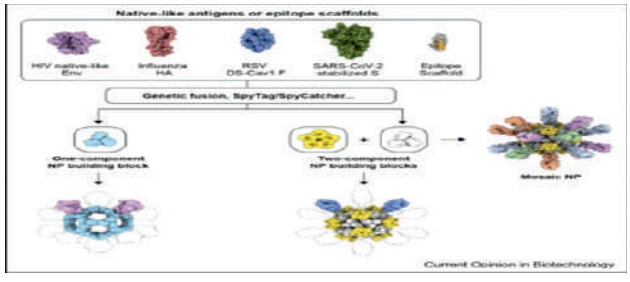

Figure 3. Schematics of vaccine immunogens developed employing a computationally designed Nano Particle (NP) system.

Epitope scaffolds (epitope highlighted in orange) and native-like antigens such as Env trimer of HIV, HA of influenza virus, F glycoprotein of RSV, and S protein of SARS-CoV-2 can be incorporated into either one-component, a schematic of native-like HIV Env trimers incorporated into or two-component, a schematic of DS-Cav1-stabilized F glycoprotein incorporated into Nano Particle (NP) building blocks via genetic fusion or SpyTag/SpyCatcher). It also allows production of mosaic NPs incorporating heterotypic immunogens, a quadrivalent influenza NP vaccine candidate employing the two-component

system. Figure 3. shows schematics of vaccine immunogens developed employing a computationally designed NP system.

Computational Engineering Perspective

From a bioengineering standpoint, structural bioinformatics represents an exemplar of computational systems design. Modern algorithms leverage graph-based neural networks and attention-transformer architectures to infer residue–residue contacts directly from sequence embeddings. Parallel computing on GPU clusters and cloud-based infrastructures (e.g., AWS, Google Cloud Life Sciences) facilitates large-scale molecular docking and MD simulations.

Furthermore, data integration frameworks synthesise multi-omics layers—genomics, proteomics, and structural proteome data—into unified predictive models. In this respect, vaccine design increasingly resembles classical systems engineering: iterative design–simulation–validation cycles, guided by quantitative feedback. Structural bioinformatics thus transforms immunology from an observational discipline into a predictive and design-oriented science.

Challenges and Limitations

Despite its transformative capacity, structural bioinformatics encounters several epistemic and technical constraints. The accuracy of predicted structures remains contingent on the availability of homologous templates and the physicochemical realism of force fields. Additionally, antigenic variability and mutational drift, particularly in RNA viruses, can abrogate predicted epitopes, necessitating continual model retraining. The computational cost of high-resolution MD simulations—often requiring teraflop-scale resources—remains prohibitive for many research centres. Ethical considerations also arise concerning the security of genomic datasets and equitable access to computational infrastructure in low-resource settings.

Future Prospects

The imminent trajectory of structural bioinformatics will be shaped by AI-driven ensemble modelling, quantum-assisted molecular simulation, and adaptive immune-informatics pipelines. Emerging methodologies integrate cryo-EM density maps with in silico folding to achieve hybrid precision unattainable by either technique alone. Moreover, personalised vaccinology, leveraging patient-specific HLA genotypes, is poised to deliver bespoke immune-therapeutics tailored through computational epitope optimisation. The confluence of structural bioinformatics with synthetic biology may further enable on-demand vaccine fabrication through programmable DNA assembly—a vision where computational models directly instruct cellular manufacturing systems.

Conclusion

Structural bioinformatics has redefined the epistemological and methodological foundations of vaccine design. By embedding atomic-scale computation within the bioengineering workflow, it enables the rational construction of immunogens that are structurally stable, antigenically potent, and swiftly translatable to clinical practice. The discipline epitomises the synthesis of data, structure, and design, transforming the biological narrative into an engineering problem of extraordinary precision. As the boundaries between computation and biology continue to dissolve, structural bioinformatics will remain the linchpin of a new era in rational vaccine engineeringwhere immunity itself is no longer discovered but designed.

References

[1] K. M. Castro, A. Scheck, S. Xiao, and B. E. Correia, "Computational design of vaccine immunogens," Curr. Opin. Biotechnol., vol. 73, pp. 1–8, 2022.

[2] D. R. Bentley, S. Balasubramanian, H. P. Swerdlow, A. J. Smith, J. Milton, and C. G. Brown, "Data ethics and equitable access in computational genomics," Nat. Biotechnol., vol. 40, no. 9, pp. 1305–1312, 2022.

[3] K. S. Corbett et al., "Evaluation of the mRNA-1273 vaccine against SARS-CoV-2 in nonhuman primates," N. Engl. J. Med., vol. 383, no. 16, pp. 1544–1555, 2020.

Prachi Pratyasha Das
5th Sem, Dept. of EE

Hydroponic Farming

Now-a-days, food-growing techniques depend heavily on pesticides and chemicals, which negatively impact the water and soil. This causes water and soil pollution, large-scale depletion of the top soil and speeds up climate change. The corresponding phenomena related to it are affecting the ability of the land to grow crops, leading to worldwide food shortages. In recent years, agricultural practices have seen a major shift towards sustainable food-growing methods, including permaculture, crop rotation, polyculture, and hydroponic farming.

For a plant to grow, three things are crucial: sunlight, water, and nutrients. In a traditional setting, plants are grown in the soil, which acts as a medium through which they get the required nutrients and water. Hydroponic plants get all the essential nutrients through a solution that reaches the roots. It refers to a method of growing crops without soil. This may sound counterintuitive since plants derive essential nutrients for their growth from the soil, without which they could possibly die. Hydroponic plants, however, get all the required nutrients from a water solution medium, so the presence of soil becomes unnecessary for its survival.

One of the major benefits of hydroponic farming is that this method can be used in small- as well as large-scale settings. People who do not have a large space, such as those who live in apartments or do not have a garden, can successfully use hydroponics to grow plants. Although hydroponics is gaining positive traction among the plant growers for providing a sustainable way of cultivating food, there are some plants that do not grow properly in a hydroponic setting; which include potatoes, plants that grow tall, and vines as they have deep roots.

Source: https://earth.org/hydroponic-farming/

Gesture-Driven System Control using GMK-3: A Hybrid CNN Approach

Abstract *– Gesture-controlled systems are gaining traction in today's era of touchless technology and advanced human-computer interaction. This work presents a novel approach that uses Python, Open Sorce Computer Vision (OpenCV), and MediaPipe to control screen volume, brightness, and mouse pointer location in real-time through hand gestures. A webcam captures live video, while OpenCV handles image processing to detect and interpret hand motions effectively. The system supports three primary gestures: an open hand adjusts volume and brightness, a closed fist deactivates controls, and a pointing gesture enables mouse navigation. A denoising algorithm is implemented to enhance the signal-to-noise ratio, ensuring higher accuracy and stability in real-time usage. Furthermore, a custom dataset of hand gestures was used to train convolutional neural networks (CNNs), including Visual Generating Group (VGG16, VGG19), and Resident Network 50 (ResNet50). The best-performing model was selected for deployment, offering high precision in gesture recognition. This hands-free interface is especially valuable in scenarios where physical contact is impractical or for users with limited hand mobility. By translating natural gestures into system commands, it creates an intuitive and accessible user experience. The project marks a significant advancement in computer vision and user interface design, with promising applications in accessibility, smart homes, and broader human-computer interaction fields.*

Keywords *– Gesture recognition, CNN, VGG16, VGG19, ResNet50, OpenCV, MediaPipe*

I. Introduction

Human-computer interaction (HCI) is undergoing a significant transformation, moving beyond traditional tools like keyboards and mice toward more natural, intuitive, and touchless forms of interaction. Gesture-based control systems have emerged as a promising solution, offering enhanced convenience, accessibility, and immersive user experiences. This study presents a gesture-controlled interface that allows users to adjust screen brightness, system volume, and mouse cursor movement using simple hand gestures detected through a standard webcam. The motivation behind this system stems from practical needs in various scenarios—such as during presentations, where adjusting settings without disrupting the flow is beneficial; in sterile environments like laboratories or kitchens where physical contact should be minimized; or for individuals with physical limitations who may find traditional input devices difficult to use.The system is built using Python, leveraging the OpenCV library for real-time video capture and image processing. MediaPipe is optionally integrated to improve hand detection and tracking accuracy. The core challenge—reliable recognition of hand gestures in real-world, dynamic environments—is addressed using deep learning techniques. A custom dataset was created by capturing numerous images of three key gestures: an open hand (for adjusting volume and brightness), a closed fist (to disable controls), and a pointing gesture (for mouse navigation). This dataset was used to train multiple Convolutional Neural Network (CNN) models, including custom architectures as well as pre-trained models like VGG16, VGG19, and ResNet50 through transfer learning. To enhance the robustness of the system, denoising techniques were applied to increase the signal-to-noise ratio (SNR), resulting in improved recognition accuracy under various lighting and background conditions. Following extensive evaluation, the most effective model was selected and integrated into the live system, offering high precision and efficiency in real-time gesture recognition. This project demonstrates the powerful combination of computer vision and deep learning in developing hands-free, gesture-based interfaces. It offers a functional, user-friendly solution with broad applications in smart environments, accessibility tools, and next-generation HCI systems, emphasizing the growing importance of touchless interaction in our increasingly digital and interconnected world.

II. Related Work

Hand gesture recognition has been an active research area within Human-Computer Interaction (HCI), with diverse applications ranging from virtual controls to sign language interpretation.

In [1], the authors proposed a system combining keypoint classification and point history classification to recognize both static and dynamic gestures. By leveraging MediaPipe for landmark detection and CNNs with transfer learning, their model achieved robust pose estimation. However, the system was sensitive to occlusion and struggled with gestures from culturally diverse users.

In [2], a low-cost, webcam-based gesture control system was developed to adjust brightness and volume. It utilized fingertip distance detection between thumb and index finger to scale the output. Despite its simplicity and cost-effectiveness, the system lacked real-time feedback and error correction mechanisms, making it less reliable in dynamic environments.

The work in [3] focused on noise reduction and object localization using non-local algorithms and SSD-based detection. While it improved hand detection in noisy settings, it relied on basic Haar-cascade classifiers and did not implement real-time response metrics, limiting its applicability in interactive systems.

Another study [4] integrated gesture recognition with cloud-based IoT platforms, using UWB tracking and motion history imaging for enhanced localization. Though the system was scalable and precise, it was constrained by a static gesture set and simple algorithms, making it difficult to adapt to user-defined inputsA vision-based control system using Raspberry Pi and OpenCV was presented in [5], enabling gesture-based brightness, contrast, and volume adjustments. While affordable and functional, the system partially depended on physical devices like wearable bands and lacked dynamic adaptability and feedback loops. These works provide valuable foundations for gesture recognition systems, but share common limitations including real-time responsiveness, adaptability, and dependency on additional hardware. The proposed work addresses these gaps by offering a vision-only, hardware-independent solution optimized for real-time performance and usability.

III. Proposed Work

The proposed system focuses on implementing a real-time, gesture-based interface for controlling screen brightness, system volume, and mouse cursor movement using a standard 2D webcam. The design eliminates the need for external hardware by leveraging computer vision frameworks such as OpenCV and MediaPipe for real-time hand tracking and landmark detection. The system utilizes three predefined static gestures—open hand, closed fist, and pointing gesture—each mapped to specific control functions. A custom dataset was developed for these gestures, comprising images captured under varying lighting and positional conditions at two resolutions: 64×64 pixels for custom CNN prototyping and 224×224 pixels for pre-trained models. To enhance model generalization and robustness, extensive data augmentation was applied using geometric and photometric transformations. Multiple deep learning architectures were evaluated, including a custom-built CNN and fine-tuned transfer learning models such as VGG16, VGG19, and ResNet50. These models were trained using the TensorFlow/ Keras framework, with performance compared based on classification accuracy, categorical cross-entropy loss, confusion matrix, and Area Under the Curve (AUC) - Receiver Operating Characteristics (ROC). The system architecture integrates MediaPipe's 21-point hand landmark tracking module. For dynamic control scaling, the Euclidean distance between the thumb tip (landmark 4) and the index fingertip (landmark 8) is computed in real time. The left and right hands are independently mapped to control brightness and volume respectively, while the pointing gesture enables cursor navigation. The overall objective is to provide a robust, low-cost, and accessible solution that supports real-time gesture control with minimal latency, offering practical utility in smart environments, accessibility applications, and touchless computing interfaces.

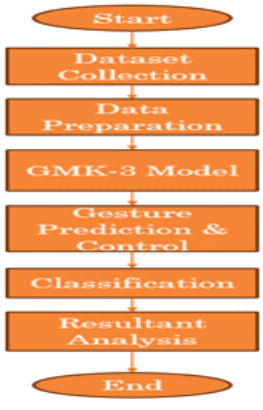

Fig. 1 System flowchart of the proposed GMK-3 gesture-driven control model

The flowchart in Figure 1 represents the systematic process of developing a gesture-driven control system using the GMK-3 model. It initiates with the collection of relevant datasets, followed by preprocessing to prepare the data for training. The GMK-3 model is then employed to learn gesture patterns and perform prediction and control tasks. These gestures are subsequently classified into predefined categories to facilitate interaction. The system's outputs are thoroughly analyzed in the resultant analysis phase to evaluate performance, accuracy, and effectiveness. This structured approach ensures each stage contributes meaningfully to achieving a reliable, real-time gesture recognition and control system for hands-free human-computer interaction.

IV. Result and Analysis

This section presents the analysis of results obtained from training and evaluating various deep learning models for real-time hand gesture recognition. All experiments were conducted on a workstation equipped with an Intel Core i7-11700H processor (2.9 GHz), 16 GB of RAM, and an NVIDIA GeForce RTX 3060 GPU with 6 GB of VRAM, running Windows 11 with Python 3.10, TensorFlow 2.11, and OpenCV 4.8 frameworks. The system achieved an average real-time processing rate of approximately 28 frames per second (FPS) during gesture recognition and control execution.

Initially, a custom Convolutional Neural Network (CNN) was trained on a dataset of 64×64 pixel images representing three gesture classes: open-hand, closed-fist, and pointing. The model achieved a validation accuracy of approximately 86.7%, with notable confusion between the pointing and closed-fist gestures, indicating limitations in resolution and model capacity. To address these issues, a custom dataset was recreated at a higher resolution of 224×224 pixels as mentioned in Table 1. This enables

Table 1. Custom Datasets Details

Feature	Initial dataset	Final dataset
Methods	Custom CNN Prototyping	Transfer Learning Models
Resolution	64*64	224*224
Classes	3	3
Target Images per Class	300	300
Actual Images	900	1200
Image Format	JPG	JPG

the use of transfer learning with pre-trained models such as VGG16, VGG19, and ResNet50. Among these, the VGG19 model demonstrated the best performance, achieving a validation accuracy of 98.33% and an AUC-ROC score of 1.00, reflecting excellent class discrimination.

The confusion matrix confirmed near-perfect classification, with minimal misclassifications and a significant improvement over the custom CNN. The system was tested for practical tasks such as controlling volume and brightness based on finger distance, and navigating the cursor through pointing gestures. Real-time operation was responsive, stable, and efficient, exhibiting minimal latency. In summary, the combination of high-resolution data, effective model architecture, and real-time integration resulted in a robust and accessible gesture-based control system that successfully addressed the challenges of earlier methods.

Figure 2 shows the AUC-ROC curve which compares the performance of different models trained on 224×224 resolution images. VGG16 and VGG19 achieved perfect classification with an AUC of 1.00, indicating excellent model performance. The CNN model showed strong results with an AUC of 0.88, while ResNet50 performed moderately with an AUC of 0.75.

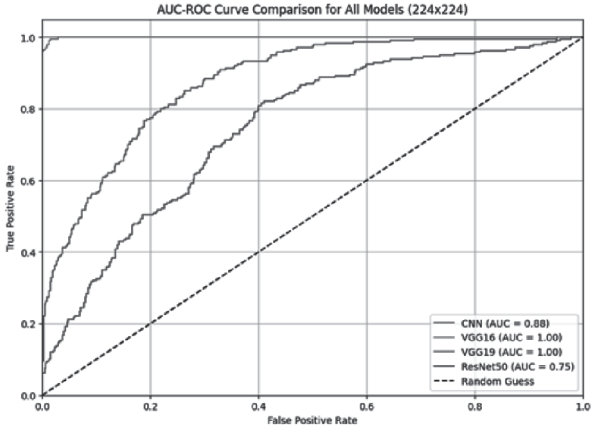

Fig. 2. Comparison of Micro-Average AUC-ROC Curves for all tested models trained on the 224x224 dataset with Learning Rate = 0.0001.

Figure 3 illustrates the training and validation accuracy trends for the VGG19 model across epochs, showing stable convergence with minimal overfitting and consistently high validation accuracy, confirming

the model's effective generalization on unseen gesture samples.

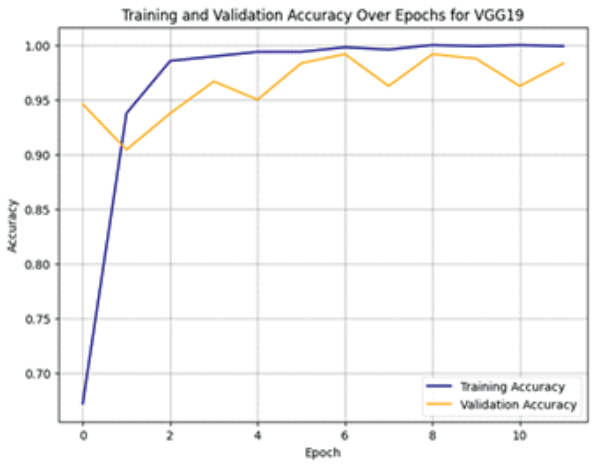

Fig. 3 Training and Validation Accuracy for VGG19

Figure 4 illustrates how to use a hand gesture experiment to increase brightness, contrast, or volume level in real time.

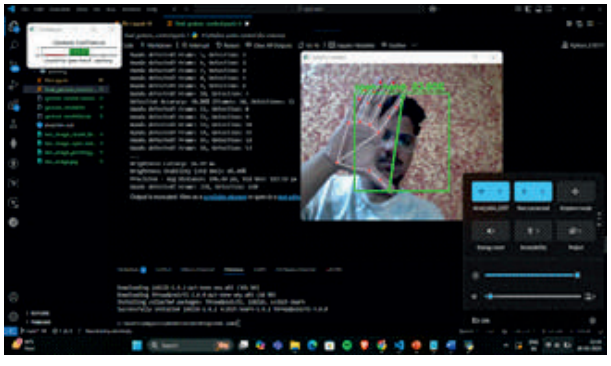

Fig. 4 Demonstrating Real-Time Hand Gesture Control System

V. Conclusion & Future Work

This work presents a vision-based, real-time hand gesture recognition system for controlling computer functionalities such as volume, brightness, and mouse navigation using a standard webcam. By integrating MediaPipe for efficient hand tracking and a fine-tuned VGG19 model for gesture classification, the system achieves high accuracy in interpreting three predefined gestures—open hand, closed fist, and pointing. The use of a custom 224×224 resolution dataset, extensive data augmentation, and comparative evaluation of deep learning models ensured robust performance under diverse conditions. Real-time responsiveness and smooth control mapping were achieved by calculating Euclidean distances between key hand landmarks. Experimental results demonstrated over 98% classification accuracy and reliable live operation, validating the system's practical viability for touchless interaction.Future enhancements include expanding the gesture vocabulary to support additional commands, integrating lightweight models such as MobileNet for edge deployment, and introducing dynamic gesture recognition using sequence models like LSTM. Improving robustness against partial occlusion, diverse lighting conditions, and unintentional gesture inputs remains a priority. Additionally, conducting formal user experience studies could help refine the system for broader adoption in accessibility, smart environments, and human-computer interaction contexts.

Acknowledgment

We would like to express our sincere gratitude to Prof. Subham Kumar Padhy, Assistant Professor, Department of Computer Science and Engineering, Silicon University, for his invaluable guidance, constant support, and expert insights throughout the course of this research.

References

[1] S. Thakur, K. Prakash, T. Bhageerath, E. Vignesh, and M. L. K. Subrahmanyam, "Real-time Hand Gesture Recognition using TensorFlow and OpenCV," International Journal of Advanced Research in Journal of Information Technology, 2024.

[2] E. S. Bandaru, S. A. Pasala, V. Pemmaraju, R. Penumaka, and S. Pilla, "Volume and Brightness Control with Hand Gestures: A Computer Vision Approach," International Journal of Novel Research and Development, vol. 8, no. 3, pp. 426–430, Mar. 2023.

[3] D. Sravani, N. T. Reddy, K. Swamy, and R. Singh, "Volume and Brightness Control Using Hand Gestures"

[4] S. Dhamodaran, P. P. Phukan, M. Singh, and S. Nandakumar, "Implementation of Hand Gesture Recognition using OpenCV," Unpublished Manuscript, 2024.

[5] N. Parimala, K. K. S. Teja, J. A. Kumar, G. Keerthana, K. Meghana, and R. Pitchai, "Real-time Brightness, Contrast and Volume Control with Hand Gesture Using Open CV Python," Unpublished Manuscript, 2023.

, **Yashwant Jena, Adyasis Maharana**
Dept. of CSE

The Coandă Effect…

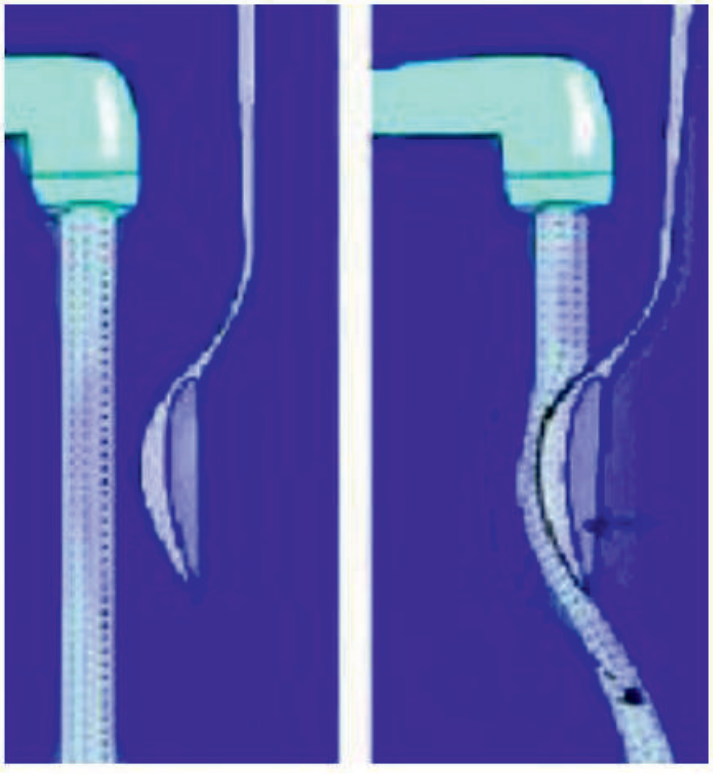

Ever wondered why a rivulet of water coming from a tap follows the curved contour of your finger, if you place it in the flow? It is due to a lesser known 'Coandă Effect', named after the Romanian Inventor Henri Coandă. The Coandă effect is the phenomena in which a jet flow attaches itself to a nearby surface and remains attached even when the surface curves away from the initial jet direction. In other words, a moving stream of fluid in contact with a curved surface will tend to follow the curvature of the surface rather than continue traveling in a straight line. This happens because of entrainment of fluid from the side away from the surface, and a lowered pressure on curved boundary.

This effect was used by Coandă in developing the first jet engine! Historically, the credit goes to Frank Whittle an English aviation engineer and Hans Von Ohain a German physicist and engineer, for developing the first working prototype of a jet engine, according to patents filed in 1928 and 1935 respectively.

However, it was Henri Coandă who developed the first 'ducted fan' jet-powered aircraft, the Coandă-1910, which he built in 1910. While the aircraft did not achieve full flight and its success is a subject of debate, his experimental jet engine demonstrated the concept of jet propulsion, and undoubtedly laid the groundwork for future jet engine development. The Coandă effect can be seen in action in lift produced by curved wing cross-sections of airplanes, and the downforce produced in Formula 1 cars. The Coandă effect is also used for thrust vectoring in spacecrafts, allowing them to change direction by having the exhaust gas follow a curved nozzle, and in life support systems in a space station to move and direct air.

(Content excerpted from Wikipedia and other web sources)

Dr. Jaideep Talukdar
Dept. of BSH

Publication Cell
Tel: 9937289499/8260333609
Email: publication@silicon.ac.in

www.silicon.ac.in

The Science & Technology Magazine

Digest

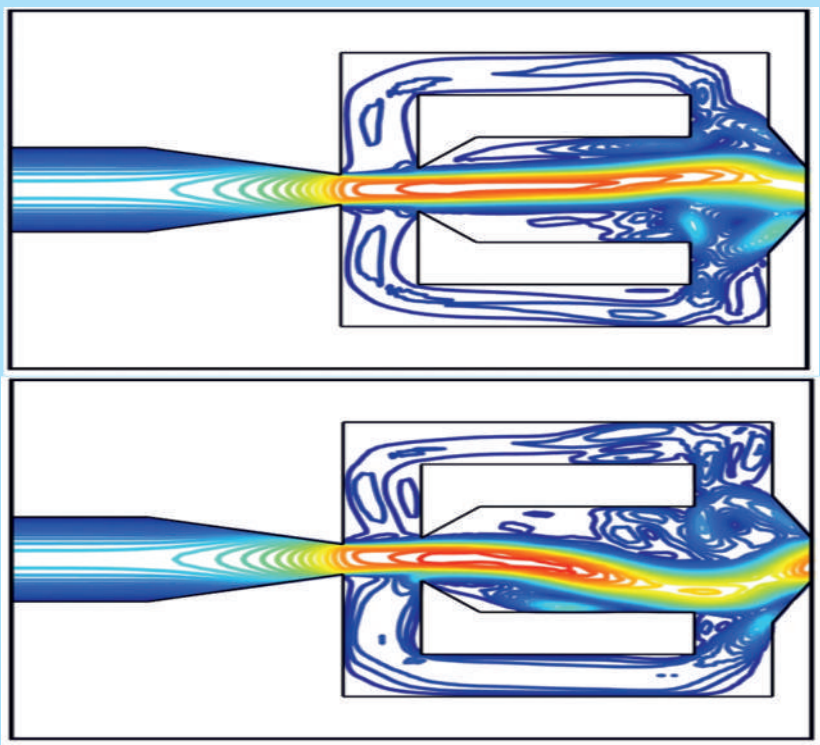

Silicon University, Odisha

Contents